

Helium compressional effect on H₂ molecules surrounded by dense H₂-He mixtures

Paul Loubeyre, René Le Toullec, and Jean-Pierre Pinceaux

*Physique des Milieux très Condensés, Université Pierre et Marie Curie,
75230 Paris Cédex 05, France*

(Received 1 August 1985)

H₂-⁴He mixtures have been studied in a diamond-anvil cell up to 8 GPa at 300 K. Phase separation has been observed and Raman spectra of the Q_1 mode of H₂ have been measured at several concentrations. For dilute H₂ in a ⁴He matrix, this mode shifts under pressure over three times faster than in pure H₂ with respect to the room-pressure frequency of the H₂ molecule. This unexpectedly large effect can be semi-quantitatively understood in terms of a collective compressional response of the He matrix on the perturbing H₂ molecule.

I. INTRODUCTION

Hydrogen and helium are the main constituents of the solar system and knowledge of the properties of their mixtures under high pressure is important for improving models of giant planets like Jupiter or Saturn.¹ Also, the understanding of their thermodynamic behavior is of theoretical interest because they are the simplest atomic and molecular species with well-known interactions. Thus a comparison of experimental and theoretical binary-phase diagrams could help to refine solid-mixture theories. It is a way to study the evolution with pressure of a diatomic molecule perturbed by a variety of condensed media, ranging from pure H₂ to H₂ highly diluted in a He matrix, that will probe different overlap and exchange effects. In this article we report the evolution of the H₂ diatomic vibrational properties, perturbed by a He environment, as a function of high pressure and He concentration: The vibrational frequency shift of H₂ and D₂ in molecular crystals at high pressure has been reported^{2,3} as a probe of the approach to metallization. The Q_1 vibrational shift of H₂ is shown to be very sensitive to He concentration. This reflects a greater compressional field acting on the H₂ molecule in a He matrix than in molecular H₂ at a given pressure.

II. EXPERIMENTAL RESULTS

The diamond-anvil cell used in the experiments is a modified version of the apparatus used previously.⁴ Here the force acting on the anvils is generated by a single-membrane bellows pressurized by helium gas which allows very sensitive pressure increments (≈ 10 MPa at 10 GPa). The setup is completely built out of hydrogen-compatible alloys (beryllium copper and stainless steel). The gas mixture is prepared at 15 MPa, where the fluidity of both components is high enough to ensure homogeneity in a reasonable time. The concentration is taken to be that of an ideal-gas mixture. The sample fluid is then compressed to 150 MPa at room temperature in the filling cell which contains the diamond-anvil cell (DAC). The diamonds are then pressed into the beryllium copper gasket by exerting an adequate overpressure on the membrane, and the setup is depressurized to room pressure while maintaining the sample sealed off in the diamond cell. The setup will be described in more detail in a forthcoming paper. The sample was typical-

ly 100 μm in diameter and 30 μm in thickness and the pressure was measured by the ruby luminescence scale, with a constant pressure coefficient of $7.57 \text{ cm}^{-1} \text{ GPa}^{-1}$. Raman activity of the Q_1 symmetric stretching mode was used as a gauge of the perturbation of the H₂ molecule. Excitation was the 488-nm line of an Ar⁺ laser focused to a 15- μm spot on the sample and its power, typically a few hundred milliwatts, was kept low enough so that no measurable temperature shift was observable. The forward scattering was analyzed by a triple 2.4-m monochromator. Phase lines were directly observed through a video circuit coupled to a microscope setup. Four mixtures and pure H₂ were studied in this series of experiments at $T = 300$ K. Shown in Fig. 1 is the variation of the Q_1 mode versus pressure, for an initial molar concentration $x = 0.67$, that is a 0.67 He : 0.33 H₂, in the homogeneous and multiphase regimes. Concentrations $x = 0.15, 0.35,$ and 0.53 were studied only in the one-phase domain. The description of the successive phase transformations with pressure can be more easily followed by reference to the H₂-He phase diagrams of Street⁵ up to 1 GPa, which can be qualitatively extrapolated to higher pressures, as recently pointed out.⁶ Our Raman measurements of pure molecular H₂ agree with those of Ref. 2; the fit of the measurements of Ref. 2 is represented by the full line in Fig. 1. The dashed lines are drawn as a guide to the eye, to join together the experimental points: Up to 5.1 GPa, the fluid is homogeneous and the Q_1 frequency is shifted upwards with respect to pure H₂. Between 5.1 and 6.0 GPa, demixing occurs into H₂-rich (F_1) and He-rich (F_2) fluids. Since the initial concentration ($x = 0.67$) is rather close to the critical one,⁶ the phase separation is only weakly discontinuous. Above 6.0 GPa, F_1 crystallizes into a solid S_1 , with an isobaric enrichment in H₂. No such discontinuity occurs on the $\sigma(P)$ locus for F_2 . At a given He concentration x , and a given pressure P , the Q_1 frequency is $\sigma(x, P)$. The ratio

$$S(x) = [\sigma(x, P) - \sigma(0, 0)] / [\sigma(0, P) - \sigma(0, 0)]^{-1} \quad (1)$$

is observed to be independent of P , at least in the range of interest, i.e., from 4 to 6 GPa; $\sigma(0, 0)$, which is the frequency of the Raman active mode of pure hydrogen at room pressure is 4155.2 cm^{-1} . Thus, the $S(x)$ ratio values for the four concentrations investigated here are plotted as stars in Fig. 2. Two more points were obtained by using the ratio of observed intensities of the Raman peaks at points B and C in Fig. 1 in the two-fluid regime which gives the H₂

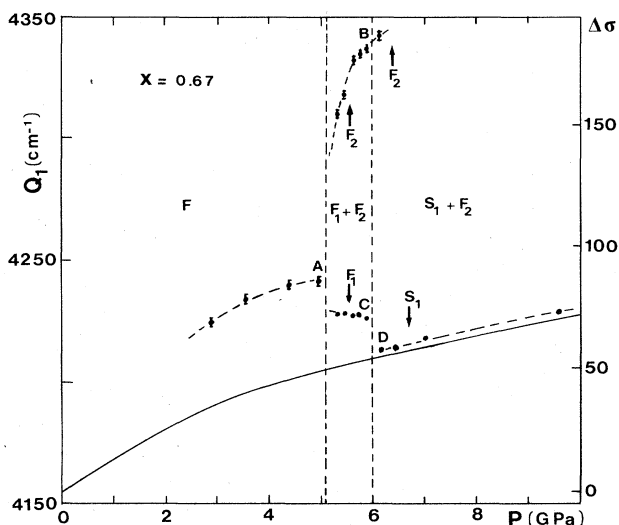


FIG. 1. Raman Q_1 vibrational frequencies of an H_2 molecule in the different phases of an initial $x = 0.67$ fluid mixture. The dots are the experimental points and the full line the results for pure molecular H_2 fitted with the polynomial form of Ref. 2.

molar concentration ratio. This ratio, together with the volume ratio (given by the ratio of areas) and the conservation of mass equation gives $x = 0.95$ at B and 0.48 at C . These two values are plotted as solid circles in Fig. 2.

In both the fluid and solid phases, the halfwidth ω of the Q_1 line (Fig. 3) strongly increases with He concentration x : from 7 cm^{-1} in the H_2 -rich solid to 60 cm^{-1} in the He-rich fluid ($x = 0.95$). Obviously, as x increases, the observed Raman signal weakens and so the error bars in Fig. 3 get larger with increasing x . The broadening is inhomogeneous

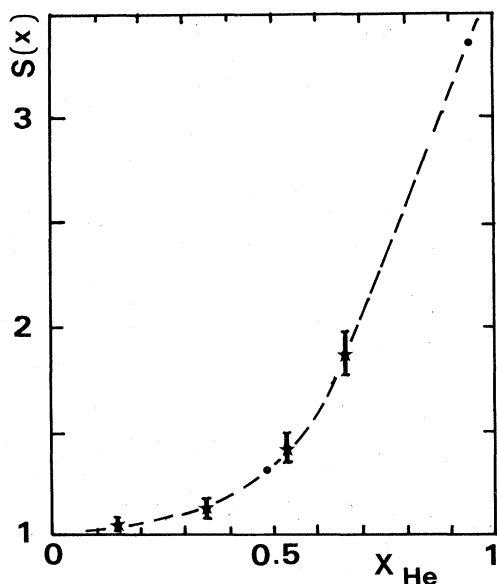


FIG. 2. Ratio of the Q_1 shift with pressure of an H_2 molecule in a mixture with He concentration x to the pure molecular one vs x [Eq. (1)]. The stars are the homogeneous fluid measurements and the dots the calculated concentrations of the separated phases of an initial $x = 0.67$ mixture.

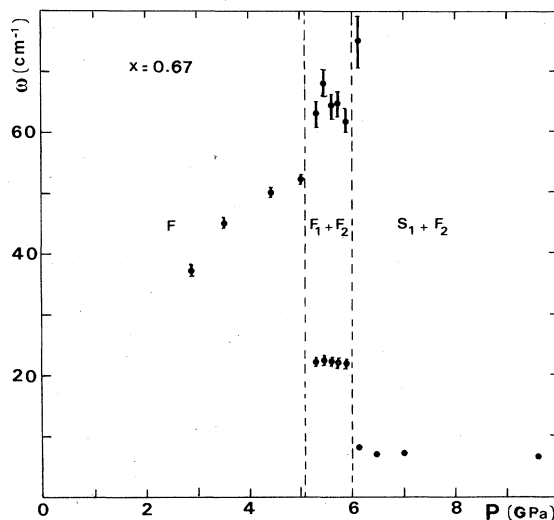


FIG. 3. Halfwidth ω of the Raman Q_1 band vs pressure (cf. Fig. 1 for the frequencies vs pressure).

because of the statistical distribution of the different environments of a given H_2 molecule.⁷ It is clear from Fig. 2 that as the average He concentration x increases, a change in the local environment of the H_2 molecule, which is equivalent to a local fluctuation of x , will induce a larger variation of the shift since $\Delta\sigma/\Delta x$ increases with x . The line shape of the Q_1 band is therefore a consequence of the curve $S(x)$ through the inhomogeneous broadening: For x around 0.5 instead of the usual Voigt profile^{7,8} the Q_1 band has a high-frequency tail, coming from the contribution of H_2 molecules surrounded by a larger local x environment, and this reflects the nonlinear variation of $S(x)$ in this domain. For larger x the band is symmetric since $S(x)$ is linear.

III. INTERPRETATION

In this paragraph we semiquantitatively account for the large frequency shift of the Q_1 mode of the H_2 molecule surrounded by dense helium, that is, for infinitely diluted H_2 , with respect to its value in pure H_2 at the same pressure. For analytical simplicity we make the following assumptions: (i) The H_2 molecule is in a substitutional site of an fcc ^4He matrix. (ii) The temperature effects can be neglected, since the thermal energy is much smaller than the compressional one. (iii) The species interact through nearest-neighbor r^{-12} potentials and the small anisotropy of the H_2 molecule is neglected.⁹ Indices 1 and 2 denote He atoms and the H_2 molecule, respectively, and ξ_{ij} is the potential constant between species i and j . Because of the scaling law of r^{-12} potentials, the nearest-neighbor distance R_1 in the fcc ^4He matrix is related to the pressure P by $R_1 = (C_3 \xi_{11}/P)^{1/15}$, where C_3 is a tabulated constant.¹⁰ The first array of He atoms around the perturbing H_2 molecule is homothetically distorted and the distortion of higher-order neighbor distances is neglected. The H_2 -He distance is $R_1(1 + \alpha)$, α being the distortion parameter; r_e is the interatomic distance within the H_2 molecule. At a given pressure P , the equilibrium parameters α and r_e are obtained by minimizing static potential energy which is a sum of the in-

tramolecular and guest-host interactions. Since H₂-He interactions are independent of r_e , this can be done independently for α and r_e . The distortion parameter α is obtained by minimizing the lattice energy

$$U(\alpha) = \sum_z \xi_{12} |\mathbf{R}_z|^{-12} + \sum_z \sum_{z'} \xi_{11} |\mathbf{R}_z - \mathbf{R}_{z'}|^{-12}, \quad (2)$$

where Z' numbers the He nearest neighbors of each of the Z H₂ nearest neighbors of the H₂ molecule. Expanding this energy to second order in α , taking into account the crystal cubic symmetries, and retaining higher-order terms only, we obtain

$$\alpha = (\xi_{12} - \xi_{11})(13\xi_{12})^{-1}. \quad (3)$$

The interatomic distance r_e in the H₂ molecule is determined by the equality of the intramolecular force and the crystal-field one F along the intramolecular axis oriented along the 100 direction, where

$$F = 24\sqrt{2}\xi_{12}[R_1(1+\alpha)]^{-13}. \quad (4)$$

Since the H₂-He interactions considered here do not depend on r_e , the vibrational frequency shift $\Delta\sigma$ is due to the anharmonicity of the intramolecular potential and it implies, according to Eq. (8) of Ref. 11, that $\Delta\sigma$ is proportional to $(r_e - r_0)$, where r_0 is the interatomic distance within an isolated H₂ molecule. Expanding the intramolecular potential energy to first order, the intramolecular force, which is equal to F , is proportional to $(r_e - r_0)$ and transitively that $\Delta\sigma$ is proportional to F . Expressing R_1 as a function of P in Eq. (4), $\Delta\sigma$ is

$$\Delta\sigma = K\xi_{12}(1+\alpha)^{-13}(P/\xi_{11})^{13/15}, \quad (5)$$

where K is a constant. This calculation for an He matrix is applicable to an H₂ matrix (pure H₂) by replacing α by 0 and index 1 by 2 in all previous equations of Sec. III. Finally, the ratio of the vibrational shift of H₂ in an He matrix to that in an H₂ one at the same pressure is simply given by

$$S(1) = \xi_{12}\xi_{22}^{-1}(1+\alpha)^{-13}(\xi_{22}/\xi_{11})^{13/15}. \quad (6)$$

Taking the usual values of r^{-12} potential constants of He-He, H₂-H₂ Lennard-Jones interactions¹² and doing a Berthelot-Lorentz combination rule¹³ (a geometrical average for the potential well depth and an arithmetical one for the hard-core diameter) for the H₂-He interaction, we obtain a dilation of the first neighbor distance $\alpha = 6\%$ and the shift ratio $S(1) = 1.5$. This is over a factor of 2 smaller than the experimental value $S(1) \approx 3.5$, since several factors have been neglected in the previous evaluation.

(i) Only nearest-neighbor interactions have been considered; next-nearest-neighbor interactions will tend to decrease $\sigma(0,p)$ and therefore increase $S(1)$. Including the

anisotropy of H₂ interactions and their dependence on r_e would go in the same direction.

(ii) The r^{-12} form is known to be too stiff: Using r^{-12} force constants that, in the density range considered, locally best approximate the known exponential potentials for helium,¹⁴ hydrogen,⁹ and H₂-He interactions,¹⁵ we get $S(1) \approx 1.8$.

(iii) Finally, the exchange and overlap effects in the H₂ solid are known to lead to an increase of the intermolecular bond and to a downward trend of the Q_1 frequency versus pressure above 40 GPa.² In our experimental pressure range (≤ 10 GPa) we assumed these effects to be taken into account by the repulsive part of the H₂ potential, but this is not valid at very high pressures where they will lead to a further increase of $S(1)$. Crude as it may be, this model gives a semiquantitative estimate of $S(1)$ and pins down the essential ingredients of this experimental fact: In the case of an H₂ molecule in an He matrix, the relative increase of the Raman frequency shift is largely due to a collective response of the He matrix to its distortion by an H₂ molecule that brings a greater compressional field on the H₂ molecule than at the same pressure in an H₂ matrix (obviously in one dimension the calculation would show no increase). Increasing the He concentration x of the surrounding medium turns on this effect as shown by $S(x)$ in Fig. 2.

IV. CONCLUSION

The properties of an H₂ molecule, surrounded by a dense H₂-He mixture, are strongly dependent on the He concentration. That leads to a surprisingly large increase (250%) of the Q_1 vibrational shift with pressure going from a pure H₂ to a pure He environment. This effect is semiquantitatively explained in terms of a larger He matrix compressional field. Complete understanding of this effect will sensitively probe the interspecies interactions which are important for models of Jovian planets. Finally, the calibration of such an effect is a useful gauge of H₂ concentrations in separated phases in high-pressure studies of H₂-He binary-phase diagrams.

ACKNOWLEDGMENTS

We thank J. M. Besson for continuous interest in this work and many helpful discussions. This work was supported in part by the Commissariat à l'Énergie Atomique Grant No. 1-617-AV-4 and by the Institut National d'Astronomie et de Géophysique. The Physique des Milieux très Condensés is "Équipe associée au Centre National de la Recherche Scientifique (U. A. 782)."

¹D. J. Stevenson, *Annu. Rev. Earth Planet. Sci.* **10**, 257 (1982).

²S. K. Sharma, H. K. Mao, and P. M. Bell, *Phys. Rev. Lett.* **44**, 886 (1979).

³I. F. Silvera and R. J. Wijngaarten, *Phys. Rev. Lett.* **47**, 39 (1981).

⁴J. P. Pinceaux, J. P. Maury, and J. M. Besson, *J. Phys. Lett.* **40**, 307 (1979).

⁵W. B. Street, *Astrophys. J.* **186**, 1107 (1973).

⁶J. A. Shouten, L. C. Van den Bergh, and N. J. Trappeniers, *Chem. Phys. Lett.* **114**, 401 (1985).

⁷H. Dubost, in *Inert Gases*, edited by M. L. Klein, Springer Series in Chemical Physics, Vol. 34 (Springer-Verlag, Berlin, 1984), p. 145.

⁸K. S. Schweitzer and D. Chandler, *J. Chem. Phys.* **76**, 2296 (1982).

⁹I. F. Silvera and V. V. Goldman, *J. Chem. Phys.* **69**, 4209 (1978).

¹⁰D. C. Wallace and J. L. Patrick, *Phys. Rev. A* **137**, 152 (1965).

¹¹R. D. Etters and A. Helmy, *Phys. Rev. B* **27**, 6439 (1983).

¹²J. O. Hirschfelder, C. F. Curtiss, and R. B. Bird, *Molecular Theory of Gases and Liquids* (Wiley, New York, 1964).

¹³R. A. Aziz, in *Inert Gases*, edited by M. L. Klein, Springer Series in Chemical Physics, Vol. 34 (Springer-Verlag, Berlin, 1984), p. 65.

¹⁴R. A. Aziz, V. P. S. Nain, J. S. Carley, W. L. Taylor, and G. T. Mc Gonville, *J. Chem. Phys.* **70**, 4330 (1979).

¹⁵K. T. Tang and J. P. Toennies, *J. Chem. Phys.* **68**, 5501 (1978).